Atomic Spectroscopy

Article

Utilizing Low Sample Uptake Rates and A Nitrogen Mixed-gas Plasma for the Elimination of Oxide-based Interferences in ICPMS Analyses

Michael G. A. Trolio and Diane Beauchemin *

Department of Chemistry, Queen's University, 90 Bader Lane, Kingston, ON K7L 3N6, Canada

Received: *August 02, 2024;* ***Revised:*** *September 25, 2024;* ***Accepted:*** *September 25, 2024;* ***Available online:*** *September 25, 2024.*

DOI: 10.46770/AS.2024.174

ABSTRACT: Spectroscopic interferences have long negatively impacted the accuracy of inductively coupled plasma mass spectrometry (ICPMS) analyses. Of these, oxide-based interferences, the combination of an analyte with oxygen producing a new ion 16 mass units greater than the original analyte, often proves most prevalent and difficult. A cheap and reliable method that permits the mitigation of oxide-based interference would be highly beneficial. Here-in, low sample uptake rate was used to reduce the formation of lanthanide oxide-based interferences in ICPMS analyses through temperature and Le Châtelier effects. Introduction of oxide forming solutions (50 μg L^{-1}) composed of lanthanide elements at 1 mL/min yielded an average oxide ratio of 4.5 ± 7.2% while introduction at 50 μL L min^{-1} yielded 0.54 ± 0.26%. A similar method using 2% nitrogen gas in the bulk plasma concurrently decreased oxide-based interferences. The benefits observed with low sample uptake rate and a mixed-gas plasma were combined to virtually eliminate oxide based-interferences for many of the lanthanide elements and provide a modest signal enhancement compared to an Ar plasma operated at a higher sample uptake rate. For example, when comparing the best oxide reduction method to the worst, oxide formation is mitigated by 97%. Of the three sample uptake rates tested, 235 μL min^{-1} under mixed-gas plasma conditions offers the best balance between the oxide interferences mitigation and signal intensity. Ultimately, low sample uptake rate may prove essential in increasing ICPMS analysis accuracy while safeguarding resources and minimizing chemical waste for generations to come.

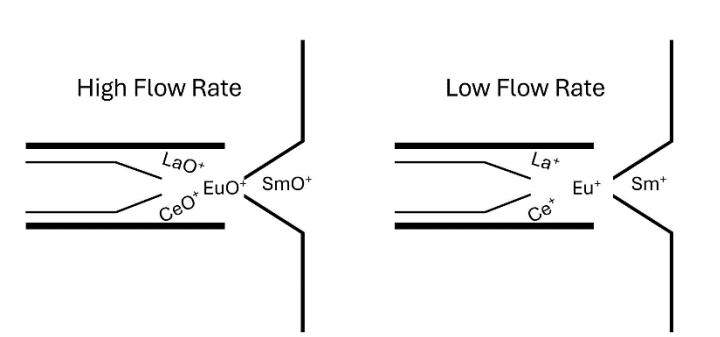

INTRODUCTION

Inductively coupled plasma mass spectrometry (ICPMS) can be found in many laboratories worldwide because it offers a wide linear dynamic range and low limits of detection. Unfortunately, ICPMS is susceptible to various interferences that can plague accuracy and precision, which can be classified as either spectroscopic or non-spectroscopic. Non-spectroscopic interferences involve analyte signal enhancement or suppression by the sample matrix. Sample transport effects and space-charge effects are two common examples of non-spectroscopic interferences.[1] An effective way to compensate for non-spectroscopic interferences is to utilize internal standardization.[1] Alternative mitigation methods include sample dilution[2] or injection of smaller sample volumes.[3]

Spectroscopic interferences may result from tailing, when adjacent mass spectra signals overlap, from polyatomic ions or doubly charged ions having the same mass-to-charge ratio (*m/z)* as that of an analyte, or from isobaric interference, when two elemental ions possess the same *m/z* (such as Fe and Ni each having an isotope at *m/z* 58). A specific example of polyatomic interference is oxide-based, when an elemental ion undergoes a

Table 1. Review of mixed-gas plasma studies in ICPMS

Authorship	Year published	Results
Lam and Horlick[10]	1990	5% N_2 addition to the outer gas flow attenuated $^{40}Ar^{16}O^+$, $^{40}Ar^{16}O^1H^+$, $^{40}Ar^{40}Ar^+$, $^{35}Cl^{16}O^+$, and $^{40}Ar^{35}Cl^+$ interferences and enhanced analyte signals up to a factor of four.
Evans and Ebdon[11]	1990	The introduction of an organic solvent (10% isopropyl alcohol in water) or a molecular gas (<5% N_2) into the central channel of the inductively coupled plasma reduced signals from $^{40}Ar^{35}Cl^+$, $^{40}Ar^{40}Ar^+$ and $^{35}Cl^{35}Cl^+$.
Lam and McLaren[12]	1990	8% N_2 in the outer gas reduced of $^{40}Ar^{16}O^+$ and $^{238}U^{16}O^+$.
Beauchemin and Craig[13]	1991	10% N_2 in the plasma reduced matrix effects caused by Na and improved the precision of the mean $^{57}Fe^+/^{56}Fe^+$ ratio measured in 0 to 0.1 M sodium solutions by a factor of 10, and that of $^{76}Se^+/^{78}Se^+$ by a factor of 4
Wang and Evans[14]	1992	1% N_2 in the outer plasma gas flow eliminated $^{40}Ar^{35}Cl^+$ and dramatically reduced $^{35}Cl^{16}O^+$ and $^{37}Cl^{16}O^+$ but minimal effects on other oxide interferents were found.
Louie and Soo[15]	1992	The addition of N_2 to the central plasma gas flow enhanced signal intensities for monitored analytes while decreasing $^{140}Ce^{16}O^+$ and $^{138}Ba^{16}O^1H^+$ interferences.
Holliday and Beauchemin[16]	2003	4% N_2 to the bulk plasma provided robust operating conditions that greatly reduced non-spectroscopic interference
Agatemor and Beauchemin[17]	2011	Small amounts of N_2 in the outer plasma flow and as a sheath gas reduced matrix effects and improved the detection limits.
Makonnen and Beauchemin[18]	2014	Small amounts of N_2 in the outer plasma gas flow and of H_2 as a sheath gas not only eliminated the studied matrix effects, but also improved the detection of several elements in the presence of a 0.1 M Na matrix.

condensation reaction with oxygen creating a new ion 16 *m/z* units greater than the original ion.[4] Oxide interferences are extremely common in ICPMS analyses but are not easily alleviated for the full suite of lanthanides without tandem mass spectrometry (ICPMS/MS). Unfortunately, ICPMS/MS is significantly more expensive than ICPMS and can generally not be afforded by many laboratories, including commercial ones.[4,5] Collision cells have been proven effective at reducing oxide interferences through the intentional addition of a gas that either modulates the *m/z* of the analyte or reacts with the interfering element to reduce the formation of oxide-based interferences. Unfortunately, reaction cells are known to reduce the sensitivity of the sample method and may not be present in older instruments that many laboratories still use and cannot afford to replace.[6,7]

Without ICPMS/MS, few mitigations methods exist for oxide-based spectroscopic interferences. Monitoring an alternative isotope not affected by oxide interferences may be considered for analytes possessing multiple isotopes, but is not feasible for the many monoisotopic elements of the periodic table.[8] Similarly, mathematical correction equations that rely on natural isotopic abundances are not always applicable and possess many drawbacks.[8] Mixed-gas plasmas, where hydrogen or nitrogen is added to one or more gas flows of the plasma, may attenuate spectroscopic interferences by facilitating a more efficient energy transfer from the bulk plasma to the central channel, allowing for a greater extent of atomization and ionization.[9] This has been demonstrated to provide relief for several oxide-based interferences (Table 1).

The beneficial decrease in oxide formation associated with N_2-containing mixed-gas plasmas is a result of nitrogen's greater thermal capacity, which reduces the size of the plasma, resulting in an increased power density of the plasma. This increased concentration of energy allows for a greater extent of ionization, increasing analyte signal for elements that are not 100% ionized in an Ar plasma.[16] Furthermore, when nitrogen is in the presence of oxygen, it reacts to form nitrogen oxide species such as nitric oxide (NO) or nitrogen dioxide (NO_2). Thus, by virtue of this 'oxygen scavenging effect', less oxygen remains available in the plasma for potential interference reactions.[19,20]

Trolio *et. al*[3,21] demonstrated that simply decreasing the volume of sample injected decreased the percent formation of CeO^+. The proposed rationale behind the observed trend is two-fold: 1) smaller sample sizes require less energy for desolvation, vaporization, and atomization, leaving more energy for complete ionization; 2) an effect related to Le Châtelier's principle reduces the likelihood of oxide condensation reactions from taking place due to lower absolute concentrations of analytes. However, a manual method that cannot easily be automated was used for the injection of as little as 1-µL aliquots.[3,21] An alternative approach that can easily be implemented is decreasing the sample uptake rate. Grotti *et al.* indeed reported a decrease in CeO^+ formation from 25% to 5% when sample uptake decreased from 80 µL min^{-1} to 10 µL min^{-1} during the total introduction of microsamples using a heated torch-integrated sample introduction system.[22]

As of now, no one has systematically focused on the application of simple methods to alleviate oxide formation. The goal of this work was to study the effect of sample uptake rate and of a N_2-based mixed-gas plasma on oxide formation by the suite of lanthanide elements. The two approaches were tested alone and in combination to find the best way to mitigate oxide formation without degrading sensitivity.

EXPERIMENTAL

Instrumentation. All measurements were accomplished using a NexION 2000B (PerkinElmer, Woodbridge, ON, Canada) quadrupole-based ICPMS instrument equipped with a Burgener SC-175 parallel path nebulizer (Burgener Research, Mississauga, ON, Canada) fitted into a cyclonic spray chamber (PerkinElmer). The optimization of the ICPMS parameters was performed using a 1 µg L^{-1} tuning solution containing Be, Mg, Co, In, Ce, Pb, and Ba in 1% HNO_3 at a sample uptake rate of 200 µL min^{-1}. The resulting ICPMS operating conditions are summarized in Table 2. In all experiments, the instrument's variable speed peristaltic pump was used in conjunction with different size peristaltic pump tubing to achieve the desired flow rates (verified by collecting samples and weighing on a micro analytical balance). A 2% addition of N_2 to the Ar plasma gas was chosen to provide an effective mixed-gas plasma[18] while ensuring environmental and financial sustainability. The mixed-gas plasma operating conditions were optimized to produce similar signal intensities to that of the Ar plasma to enable direct comparison of the oxide interference reduction effects of the mixed-gas plasma.

Reagents. Doubly deionized water (DDW) used in the preparation of the sample solutions was purified to a resistivity of 18 MΩ cm using an Atrium Pro UV/DI (Sartorius Stedim Biotech, Göttingen, German) water purification system. Serial dilution was conducted from 1000 and 10 000 mg L^{-1} mono-elemental solutions (SCP Science, Baie-D'Urfe, QC, Canada) to prepare solutions. Multiple solutions were made at 3 mg L^{-1} and 50 µg L^{-1} concentrations to prevent overlap between oxides and analytical peaks: 1) La, Ce, Pr, Nd, Sm; 2) Eu, Gd, Tb, Dy, Ho; 3) Er, Tm, Yb, Lu.

Data processing. Data were collected in time-resolved mode to permit temporal graphical representation of signal and oxides ratios (not used in this article). Excel 2016 was used for all calculations, starting with blank subtraction. Oxide interference was considered as the analyte oxide signal divided by the analyte signal (MO^+/M^+). Signal was averaged over a 15-s window. Similarly, oxide ratios were computed point-by-point and then averaged over the same 15-s window.

RESULTS AND DISCUSSION

Effect of sample uptake rate in an Ar plasma. Decreasing the sample uptake rate while introducing 50 µg L^{-1} lanthanides solutions systematically decreased sensitivity (Table S1). According to Fig. 1, the lanthanides signal at 1 mL min^{-1} is on average 3.23 ± 0.99 times that at 235 µL min^{-1} and 15.1 ± 4.7 times that at 50 µL min^{-1}. If analyte concentration is increased to 3 mg L^{-1} (Table S2), the lanthanides signal at 1 mL min^{-1} is on average 2.2 ± 1.4 times that at 235 µL min^{-1} and 6.5 ± 4.3 times that at 50 µL min^{-1}. Table S3 and Fig. 2 show a positive correlation between sample uptake rate and the formation of lanthanide oxides when introducing 3 mg L^{-1} lanthanides. As an example, an average 77 ± 13 % decrease in lanthanide oxide formation resulted when comparing trials with 3 mg L^{-1} solutions of lanthanide elements at 1 mL min^{-1} to 50 µL min^{-1}. Such positive correlation was also observed with 50 µg L^{-1} lanthanide solution (Table S4), particularly between 50 µL min^{-1} and 1 mL min^{-1}.

On average, similar oxide formation occurred at 3 mg L^{-1} and 50 µg L^{-1} (Table 3), which decreased similarly upon a decrease in

Table 2. NexION 2000B ICPMS optimized operating conditions

Parameter	Setting	
Type of plasma	Ar	Ar-N_2
Ar plasma gas flow rate (L min^{-1})	15.0	14.7
Nitrogen plasma gas flow rate (L min^{-1})	0.0	0.3
Ar auxiliary gas flow rate (L min^{-1})	1.2	1.2
Ar nebulizer gas flow rate (L min^{-1})	0.98	1.28
Plasma RF power (kW)	1.60	

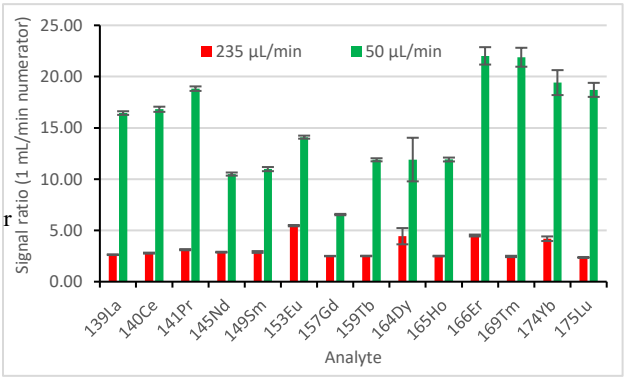

Fig. 1 Analyte signal from 50 µg L^{-1} lanthanides at 1 mL min^{-1} divided by that at 235 (red bars) or 50 (green bars) µL min^{-1} in an Ar plasma, with standard deviation as error bar (n=10).

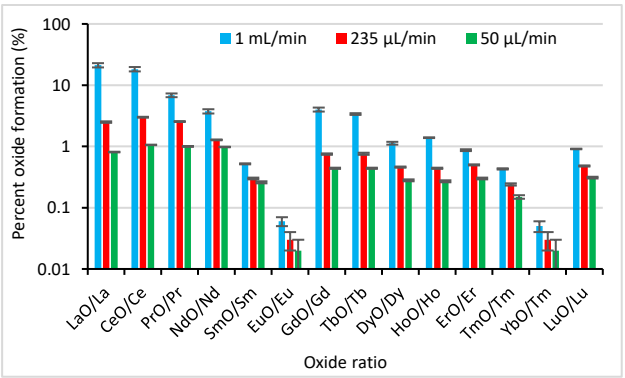

Fig. 2 Percent oxide formation of lanthanide elements with standard deviation as error bar (n=10) when introducing 3 mg L^{-1} lanthanides at different sample uptake rates in an Ar plasma.

Table 3. Average (± standard deviation) and range of oxide formation at 1000, 235, and 50 µL min^{-1} uptake rates (n = 14 elements)

Sample uptake rate (µL min^{-1})	% oxide formation at 3 mg L^{-1}		% oxide formation at 50 µg L^{-1}	
	Average	Range	Average	Range
1000	4.7 ± 6.8	0.05-21.2	4.5 ± 7.2	0.05-24.9
235	0.95 ± 0.99	0.03-3	0.92 ± 0.75	0.04-1.28
50	0.45 ± 0.36	0.02-1.06	0.54 ± 0.26	0.04-0.83

Table 4. Average percent change in oxide formation from 1 mL min^{-1} to 235 µL min^{-1} and 50 µL min^{-1} trials (n = 14 elements)

Concentration	% change to 235 µL min^{-1}	% change to 50 µL min^{-1}
3 mg L^{-1}	-61 ± 17	-75 ± 14
50 µg L^{-1}	-43 ± 48	-54 ± 32

Table 5. Average (± standard deviation) and range of oxide formation at 1 mL min^{-1}, 235 µL min^{-1}, and 50 µL min^{-1} uptake rates with a 2% N_2 mixed-gas plasma (n = 14 elements)

Sample uptake rate (µL min^{-1})	% oxide formation with 3 mg L^{-1}		% oxide formation with 50 µg L^{-1}	
	Average	Range	Average	Range
1000	1.2 ± 1.5	0.02-4.9	0.89 ± 0.91	0.02-2.8
235	0.33 ± 0.35	0.01-1.11	0.52 ± 0.36	0.01-1.72
50	0.12 ± 0.08	0.01-0.28	0.14 ± 0.21	0.01-0.32

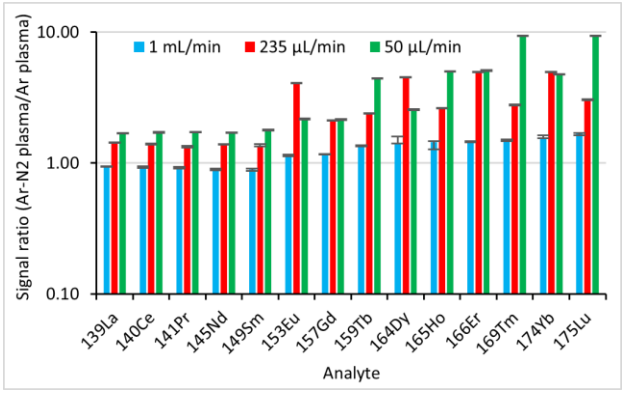

Fig. 3 Analyte signal from 50 µg L^{-1} lanthanides in a 2% N_2 mixed-gas plasma divided by that in an Ar plasma at each of 1 mL min^{-1} (blue bars), 235 µL min^{-1} (red bars) or 50 µL min^{-1} (green bars), with standard deviation as error bar (n=10).

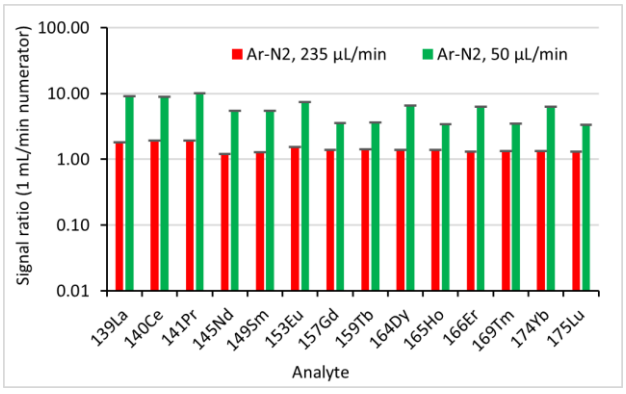

Fig. 4 Log of analyte signal from 50 µg L^{-1} lanthanides at 1 mL min^{-1} divided by that at 235 (red bars) or 50 (green bars) µL min^{-1} in a 2% N_2 mixed-gas plasma, with standard deviation as error bar (n=10).

sample uptake rate. These results reaffirm the low sample volume cerium oxide experiments previously reported by Trolio *et al.*[3, 21] Because the formation of oxides is known to depend on plasma temperature,[11] when sample uptake rate is reduced, less plasma energy is exhausted on evaporation and desolvation, leaving more energy for atomization and ionization. Indeed, the maximum sample load is known to change with the radio frequency power of the ICP;[23] thus, the stability of the plasma is dependent on the sample load at a given plasma power. An effect related to Le Chatelier's principle may also be taking place. At lower sample uptake rate, lanthanide elements occupy a smaller volume within any portion of the ICPMS instrument, resulting in the absolute concentration of analyte in space decreasing. Hence, the probability of oxide-forming collisions and reactions is reduced. This is supported by the dependence of oxide formation on concentration in Table 4: the decrease in oxide formation is greater at 3 mg L^{-1} than at 50 µg L^{-1}. In other words, with large sample uptake rate Ar trials, more oxides form due to relatively low plasma temperatures and Le Châtelier concentration effects. Indeed, as sample uptake rate decreased, oxide formation decreased. Thus, more oxides are experienced at 1 mL min^{-1} than at 50 µL min^{-1}.

A desolvation system was not tested in this work because it would exacerbate matrix effects by removing the load buffer effect of water, which is not practical for the analysis of a wide variety of samples with complex matrices. One aim of this study was indeed to find a simple method that can easily be implemented by analytical service laboratories.

Effect of a 2% N_2 mixed-gas plasma. The addition of 2% N_2 in the Ar plasma outer gas flow, in combination with optimization of the Ar nebulizer gas and Ar auxiliary gas flow rates, resulted in similar or higher analyte signal than obtained with an Ar plasma (Tables S5 and S6 versus Tables S1 and S2 respectively). This is illustrated in Fig. 3 using 50 µg L^{-1} solutions. Whereas analyte signal in the mixed-gas plasma is on average 1.23 ± 0.28 times that in the Ar plasma at 1 mL min^{-1}, it is 2.8 ± 1.3 that in the Ar plasma at 235 µL min^{-}. However, at 50 µL min^{-1}, analyte signal for all the lanthanides in the mixed-gas plasma is on average 3.8 ± 2.7 that in the Ar plasma. The greater observed signal enhancement at 50 µL min^{-1} supports the claim that smaller sample uptake rates leave more thermal energy in the plasma once ionization has occurred. It remains that, in the mixed-gas plasma, analyte signal at 235 µL min^{-1} is similar or higher than that at 1 mL min^{-1}, which is 6.0 ± 2.3 times that at 50 µL min^{-1} (Fig. 4).

In addition to increased or similar analyte signal in a mixed-gas plasma compared to an Ar plasma at a given sample uptake rate, the extent of oxide formation of lanthanide elements was substantially reduced with 2% N_2 (Tables S7 and S8). Table 5 summarizes the average percent oxide formation for lanthanide elements at the three sample uptake rates and two solution

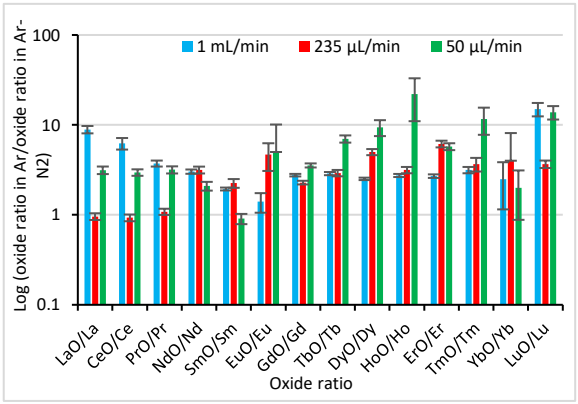

Fig. 5 Log of the oxide ratio from 50 µg L^{-1} lanthanides in an Ar plasma divided by that in a 2% N_2 mixed-gas plasma at each of 1 mL min^{-1} (blue bars), 235 µL min^{-1} (red bars) or 50 µL min^{-1} (green bars), with standard deviation as error bar (n=10).

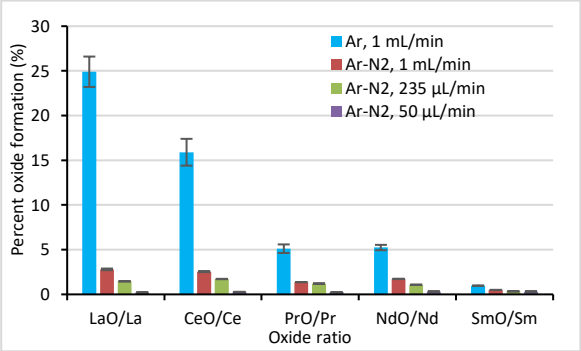

Fig. 6 Extent of oxide formation while introducing 50 µg L^{-1} of lanthanide elements in an Ar plasma at 1 mL min^{-1} (blue bars) and in a 2% N_2 mixed-gas plasma at 1 mL min^{-1} (red bars), 235 µL min^{-1} (green bars) and 50 µL min^{-1} (purple bars) with standard deviation as error bar (n=10).

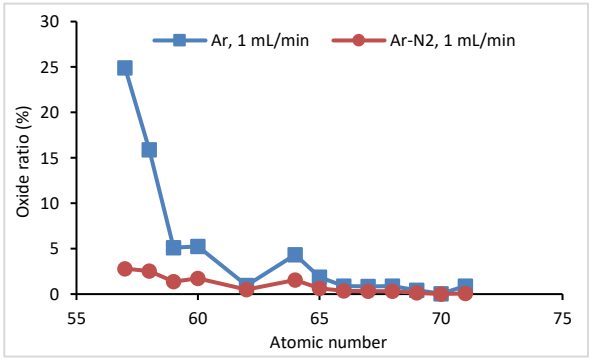

Fig. 7 Oxide formation as a function of atomic number while introducing 50 µg L^{-1} of lanthanide elements at 1 mL min^{-1} in an Ar plasma and in a 2% N_2 mixed-gas plasma, with standard deviation as error bar (n=10).

Table 5. Average (± standard deviation) and range of oxide formation at 1 mL min^{-1}, 235 µL min^{-1}, and 50 µL min^{-1} uptake rates with a 2% N_2 mixed-gas plasma (n = 14 elements)

Sample uptake rate (µL min^{-1})	% oxide formation with 3 mg L^{-1}		% oxide formation with 50 µg L^{-1}	
	Average	Range	Average	Average
1000	1.2 ± 1.5	0.02-4.9	1000	1.2 ± 1.5
235	0.33 ± 0.35	0.01-1.11	235	0.33 ± 0.35
50	0.12 ± 0.08	0.01-0.28	50	0.12 ± 0.08

concentrations with a 2% N_2 mixed-gas plasma. Comparison of Table 5 to Table 3 indicates that the average oxide formation is systematically lower than in the Ar plasma. This is illustrated in Fig. 5 for a 50 µg L^{-1} solution, which shows the oxide ratio in an Ar plasma divided by the oxide ratio at the same sample uptake rate in a 2% N_2 mixed-gas plasma. Table 6 summarizes the results at two concentrations. On average, the oxide ratio in a 2% N_2 mixed-gas plasma is at the most one third of that in an Ar plasma. The reported signal enhancement and oxide interference reduction while utilizing a mixed-gas plasma are supported by previously reported literature that was highlighted in Table 1, especially the study by Lam and Horlick.[10]

In the case of the lanthanides having the greatest tendency to form oxides (*i.e.*, La, Ce, Pr, Nd and Sm), a dramatic decrease in the formation of oxides resulted when using a 2% N_2 mixed-gas plasma at 235 µL min^{-1} or 50 µL min^{-1} compared to an Ar plasma at 1 mL min^{-1} sample uptake rate, as shown in Fig. 6. In fact, at 50 µL min^{-1} in the mixed-gas plasma, the average oxide formation is mitigated by 97% compared to that in an Ar plasma at 1 mL min^{-1}. However, whereas the percentage of La oxide in 50 µg L^{-1} was 24.9 % in an Ar plasma at 1 mL min^{-1}, elements such as Tm and Yb only experienced 0.41% and 0.05% oxide formation respectively under the same conditions. This difference may be partly explained through the concept of lanthanide contraction. Due to 5s and 5p orbital penetration of the 4f orbital, 4f electrons are not shielded from nuclear charge as one expects with electrons in s, p, and d orbitals. Essentially, atomic radius decreases across the lanthanide elements more greatly than for other series in the periodic table.[24] The reactivity of lanthanides with oxygen may thus be expected to decrease as ionic radius decreases and nuclear charge increases. Thus, the discrepancy between the extent of oxide interference reduction amongst different lanthanides (*e.g.,* La and Ce vs Tm and Yb) may be explained by this trend, as some lanthanides are more likely to form oxides than others in the first place. However, this is not the only factor at play. Otherwise, the oxide fraction would be linearly related to the atomic number, which is not the case, as can be seen in Fig. 7.

Compared to an Ar plasma at 1 mL/min sample uptake rate, the mixed-gas plasma at 235 µL min^{-1} is clearly advantageous, as the signal is similar or higher for the majority of lanthanides (Fig. 8) and oxide formation is simultaneously reduced by 8.1 ± 1.0 fold on average. Using a sample uptake rate of 50 µL min^{-1} into the mixed-gas plasma further reduces oxide formation, by 26 ± 31 fold on average, but at the expense of sensitivity. Indeed, the analyte signal is then smaller than that in an Ar plasma at 1 mL/min by up to an order of magnitude (not shown). However, such sacrifice may be warranted in cases where the interferences caused LaO^+, CeO^+, *etc.*, which depend on sample matrix, cannot be easily corrected and lead to inaccurate results.

Furthermore, a strong positive correlation (R^2=0.97) resulted

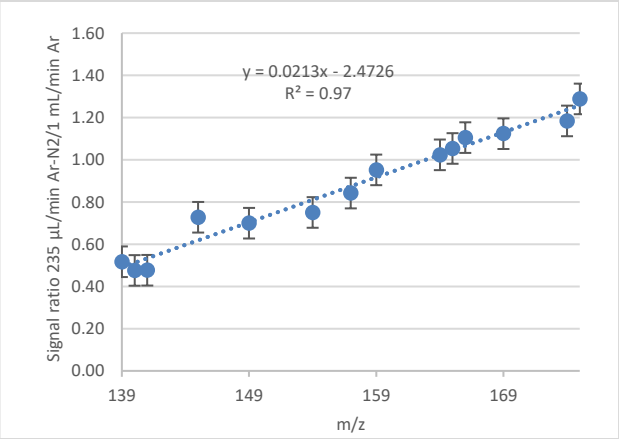

Fig. 8 Ratio of the analyte signal from 50 µg L^{-1} in a 2 % N_2 mixed-gas plasma at 235 µL min^{-1} sample uptake rate divided by that in an Ar plasma at 1 mL min^{-1}, with standard deviation as error bar (n=10).

between analyte signal ratio (235 µL min^{-1} Ar-N_2 over 1 mL min^{-1} Ar) and analyte mass (Fig. 8). Again, this may be attributed to lanthanide contraction where analytes experiencing greater lanthanide contraction benefit more from the higher thermal density of the mixed-gas plasma. In other words, as valence electrons experience a stronger attraction to the lanthanide positive nuclei (arising from increased orbital contraction), they are harder to extract in an Ar plasma as compared to a mixed-gas plasma. This trend is affirmed when plotting the same signal ratio against lanthanide element's first ionization potential. Here, a similar, yet weaker, correlation is found (see Fig. S1). To the best of the authors' knowledge, this is the first time this effect is recorded in literature. This trend, seen in both Fig. 8 and Fig. S1, further supports the notion that a higher plasma energy density is responsible for the observed reduction in oxide-based interferences at lower sample uptake rates.

The above results were reproducible over several full days of ICPMS operation, which is consistent with the absence of signal degradation reported with mixed-gas plasmas in the literature. It should be noted that the sample uptake rates chosen for this experiment may not be the optimal for real world applications. Instrument operators should optimize operating conditions for an acceptable compromise between sensitivity and oxide interference mitigation for their specific applications.

CONCLUSION

This research demonstrates a positive correlation between sample uptake rate and oxide formation across lanthanide elements. The temperature of the plasma, as well as the concentration of analyte within any part of the ICPMS instrument, may account for this effect. Injections at 235 µL min^{-1} under mixed-gas plasma conditions offered the best balance between the removal of oxide interferences and signal intensity. It was further found that the atomic number of lanthanide elements inversely correlated with oxide interference formation. A decrease in reactivity relating to lanthanide contraction may partly explain this observed trend.

By mitigating the formation of oxide-based interferences in ICPMS analysis, sample throughput may dramatically increase while diminishing downtime for ICPMS instrument maintenance compared to methods using larger sample uptake rates. Without cheap and effective mitigation methods, analysis time and cost of business increase, ultimately decreasing business profitability, with a concurrent increase in energy waste and resource mismanagement following. Indeed, the low sample uptake rate research here-in would aid to reduce the accumulation of waste on instrumental parts that require costly replacement. Furthermore, small sample uptake rate analysis would reduce waste, making this approach greener than methods using larger sample uptake rates. By understanding universal basic mitigation techniques, chemical waste can thus be reduced, and resources preserved for future generations.

Future work will expand the number of analytes and include other element groups, particularly those with a similar tendency to form oxide. Various sample types will also be considered to assess how broadly applicable a mixed-gas plasma in combination with a reduced sample uptake rate is.

ASSOCIATED CONTENT

Supporting information (Tables S1-S8, and Fig. S1) is available at www.at-spectrosc.com/as/home

AUTHOR INFORMATION

Diane Beauchemin received her Ph.D. in 1984 from Université de Montréal. She is a professor (Full) at Queen's University. Her research efforts are focused on inductively coupled plasma mass spectrometry (ICPMS) and ICP optical emission spectrometry (OES) from both fundamental and application perspectives and expanding the range of application of ICPMS/OES to geochemical exploration, risk assessment of food safety, characterization of nanoparticles, and forensic analysis. She is on the editorial board for *Atomic Spectroscopy*. Diane Beauchemin won the Alan Date Memorial Award (1988) from VG Elemental, the Distinguished Service Award (2001) from Spectroscopy Society of Canada, the Maxxam Award (2017) and Clara Benson Award (2019) from Canadian Society for Chemistry, the Gerhard Herzberg Award (2018) from the Canadian Society for Analytical Sciences and Spectroscopy, and the Environment Division Research and Development Dima Award from the Chemical Institute of Canada (2024). She is author or co-author of over 183 articles published in peer-reviewed scientific journals.

Corresponding Author

*D. Beauchemin

Email address: diane.beauchemin@queensu.ca

Notes

The authors declare no competing financial interest.

ACKNOWLEDGMENTS

The authors gratefully acknowledge the Natural Sciences and Engineering Council of Canada (NSERC) for funding (grant number CRDPJ 503887-16). MGAT also thanks NSERC for a scholarship and Queen's University School of Graduate Studies for a graduate award.

REFERENCES

1. F. Vanhaecke, *Talanta*, 1992, **39**, 737–742. https://doi.org/10.1016/0039-9140(92)80088-u
2. E. McCurdy, *Spectroscopy*, 2019, **34**, 31–33. https://www.spectroscopyonline.com/view/icp-ms-essential-steps-optimize-matrix-tolerance
3. M. G. Trolio, G. Shearing, and D. Beauchemin, *Atom. Spectrosc.*, 2023, **44**, 8–13. https://doi.org/10.46770/as.2023.013
4. E. Bolea-Fernandez, L. Balcaen, M. Resano, and F. Vanhaecke, *J. Anal. At. Spectrom.*, 2017, **32**, 1660–1679. https://doi.org/10.1039/C7JA00010C
5. R. S. Amais, A. Virgilio, D. Schiavo, and J. A. Nóbrega, *Microchem. J.*, 2015, **120**, 64–68. https://doi.org/10.1016/j.microc.2015.01.008
6. S. D. Tanner, V. I. Baranov, and D. R. Bandura, *Spectrochim. Acta B*, 2002, **57**, 1361–1452. https://doi.org/10.1016/S0584-8547(02)00069-1
7. A. Yu. Leikin, V. K. Karandashev, S. V. Lisovskii, and I. A. Volkov, *Inorg. Mat.*, 2015, **51**, 1389–1393. https://doi.org/10.1134/s0020168515140095
8. S. Wilschefski and M. Baxter, *Clin. Biochem. Rev.*, 2019, **40**, 115–133. https://doi.org/10.33176/aacb-19-00024
9. D. Beauchemin and J. M. Craig, *Spectrochim. Acta B*, 1991, **46**, 603–614. https://doi.org/10.1016/0584-8547(91)80064-A
10. J. W. H. Lam and G. Horlick, *Spectrochim. Acta B*, 1990, **45**, 1313–1325. https://doi.org/10.1016/0584-8547(90)80185-L
11. E. H. Evans and L. Ebdon, *J. Anal. At. Spectrom.*, 1990, **5**, 425–430. https://doi.org/10.1039/JA9900500425
12. J. W. Lam and J. W. McLaren, *J. Anal. At. Spectrom.*, 1990, **5**, 419. https://doi.org/10.1039/JA9900500419
13. D. Beauchemin and J. M. Craig, *Spectrochim. Acta B*, 1991, **46**, 603–614. https://doi.org10.1016/0584-8547(91)80064-a
14. J. Wang, E. H. Evans, and J. A. Caruso, *J. Anal. At. Spectrom.*, 1992, **7**, 929. https://doi.org/10.1039/JA9920700929
15. H. Louie and S. Y.-P. Soo, *J. Anal. At. Spectrom.*, 1992, **7**, 557. https://doi.org/10.1039/JA9920700557
16. A. E. Holliday and D. Beauchemin, *J. Anal. At. Spectrom.*, 2003, **18**, 1109–1112. https://doi.org/10.1039/B303184E
17. C. Agatemor and D. Beauchemin, *Spectrochim. Acta B*, 2011, **66**, 1–11. https://doi.org/10.1016/j.sab.2010.11.011
18. Y. Makonnen and D. Beauchemin, *Spectrochim. Acta B*, 2014, **99**, 87–93. https://doi.org/10.1016/j.sab.2014.06.015
19. E. H. Evans and L. Ebdon, *J. Anal. At. Spectrom.*, 1990, **5**, 425. https://doi.org/10.1039/JA9900500425
20. J. Kofsky and D. Beauchemin, *Spectroscopy*, 2020, **35**, 22-27. https://www.spectroscopyonline.com/view/improvement-limits-detection-p-s-and-ca-nanoparticle-size-absence-dissolved-analyte-using-mixed-gas
21. M. Trolio, M. Hassan, R. Oleschuk, and D. Beauchemin, *Atom. Spectrosc.*, 2023, **44**, 191–197. https://doi.org10.46770/as.2023.101
22. M. Grotti, F. Ardini, and J. L. Todolì, *Anal. Chim. Acta*, 2013, **767**, 14–20. https://doi.org/10.1016/j.aca.2013.01.017
23. T. Liu, E. Bolea-Fernandez, and F. Vanhaecke, *Spectrochim. Acta B*, 2022, **198**, 106546. https://doi.org/10.1016/j.sab.2022.106546
24. S. C. Bart, *Inorg. Chem.*, 2023, **62**, 3713–3714. https://doi.org/10.1021/acs.inorgchem.3c00440